Alkali-activation of marble sludge: Influence of curing conditions and waste glass addition

Boosting the performance of energy harvesters subject to white Gaussian vibrations through impedance matching solutions

Kailing Song
IUSS, Univ. School for Adv. Studies, Pavia, Italy,
and Politecnico di Torino, Turin, Italy
kailing.song@polito.it

Michele Bonnin
Dept. of Electronics and Telecommunications
Politecnico di Torino, Turin, Italy
michele.bonnin@polito.it

Fabio L. Traversa
MemComputing Inc.
San Diego, CA, USA
ftraversa@memcpu.com

Fabrizio Bonani
Dept. of Electronics and Telecommunications
Politecnico di Torino, Turin, Italy
fabrizio.bonani@polito.it

***Abstract*—We discuss models of piezoelectric energy harvesters for scavenging energy from random mechanical vibrations, represented by a white Gaussian noise source. We show that circuit theory can be applied to design a matching network, to be interposed between the piezoelectric transducer and the load, able to increase the power transferred to the latter. The second order matching network is compared with a previously proposed solution, based on power factor correction, implemented through a single reactive element. We show that the new architecture boosts the harvested power with respect to the simple, unmatched resistive load, by a factor larger than 9, and with respect to the power factor correction solution by more than 17%.**

***Index Terms*—Energy harvesting, piezoelectric energy harvester, nonlinear dynamical systems, equivalent circuits, load matching, power efficiency, nonlinear resonance**

I. Introduction

Environmental energy scavenging [1]–[5] is an increasingly popular solution to the issue of power supply for the wireless-connected electronic and electro-mechanical systems, constituting the hardware backbone of the Internet of things (IoT) paradigm in terms of sensors and actuators. Such solution overcomes all of the main limitations of traditional approaches, namely the use of batteries, as the latter still exhibit size and weight issues, a limited lifetime, an environmentally hazardous disposal, and ultimately a difficult maintenance as the IoT devices are scattered over large and often remote areas.

Possible ambient energy sources to be tapped for IoT device powering are quite varied, including e.g. dispersed electromagnetic waves, ambient heat, and kinetic energy from parasitic mechanical vibrations. Mechanical energy sources are especially interesting, as they are widely available as well as characterized by a relatively large power density. Parasitic vibrations are ubiquitous in mechanical structures, due to impacts or periodic motions, in buildings and bridges, due to traffic and wind, in vehicles, due to road asperity and engine induced vibrations, as well as in the very human body motion [6]–[9].

Irrespective of the source nature, energy harvesting system performance are limited by the relatively small available power densities, and by geometric constraints that impact on the frequency range where the energy conversion mechanism may effectively take place. Trading off among competing requirements is, as usual, the signature of any energy harvesting system design. For example, energy harvesters must be characterized by a sufficiently large Q factor, to convert mechanical energy into electrical power with good efficiency. However, a large Q factor is usually obtained at the expense of bandwidth, thus implying that the efficiency abruptly drops outside of a limited frequency interval. Therefore, the harvester's resonance frequency should match the spectral range where most vibrational energy is concentrated. Unfortunately, the general rule is that the smaller is the size of an object, the larger its resonance frequency will be. As a consequence, it is quite hard to realize energy harvesters that are both miniaturized, and that work efficiently at the typical frequencies of ambient mechanical vibrations. Another limiting key factor is the impedance mismatch between the mechanical and electrical domains of the harvester, and the load, often represented by an electrical or electronic circuit.

With reference to load mismatch, we have recently shown that circuit theory may represent an instrumental tool, to design solutions aimed at improving the performances of energy harvesters [10]–[13]. In this contribution, we extend our previous results on the application of circuit theory concepts, namely equivalent circuit modelling, power factor correction and impedance matching, to the design of highly efficient energy harvesting systems based on piezoelectric energy conversion. Furthermore, as from the modeling point

978-1-6654-8537-1/22/$31.00

of view mechanical vibrations are effectively represented by stochastic processes, we consider energy harvesters subject to Gaussian white noise sources that represent random mechanical vibrations. We use mechanical-to-electrical analogies to develop equivalent circuit models for the energy harvesters. As the main contribution, we show that impedance matching theory can be used to design two-port matching networks, that can be interposed between the piezoelectric transducer and the load, to maximize the power transferred to the load. We compare the performances of the new matching network to the ones of previously proposed solutions, based on a simple power factor correction scheme [11], [12]. We show that, with respect to the simple resistive load, the new architecture increases the harvested power by a factor of nine, and with respect to the power factor correction-based solution by more than 17%.

This paper is organized as follows: Section II is devoted to the description of the model we develop for the piezoelectric energy harvester, and to the derivation of the corresponding equivalent electrical circuit excited by a stochastic generator representing mechanical vibrations. The analysis of the system performance, the design of the power factor correction and of the two-port, second order matching network, and their comparison are discussed in Section III. Finally, conclusions are drawn in Section IV.

II. Energy harvesting system modelling

Besides traditional sources, i.e. solar and wind power, energy is found in the ambient in various form, such as thermal gradient, dispersed electromagnetic waves and parasitic mechanical vibrations. Although negligible at the macro-scale, these sources may be significant enough to supply power to wireless miniaturized electronic systems [14].

Ambient vibrations can be converted into usable electrical power exploiting different physical principles. The most widespread type of transducers uses the piezoelectric effect, to convert stress and strain produced by vibrations in a cantilever structure, into electrical power [4]. A schematic representation of a piezoelectric energy harvesting system for ambient mechanical vibration is shown in figure 1. A cantilever beam is fixed at one end to a vibrating support, with an inertial mass m placed at the opposite end, aimed at increasing the oscillation amplitude. The beam is covered by layers of piezoelectric material, that convert mechanical stress and strain induced in the beam by oscillations, into an electrical current. The main contribution of this work is the interposition of a properly designed, two port matching network, between the piezoelectric transducer and the electrical load. The role of the matching network is to reduce as much as possible the impedance mismatch between the electrical and the mechanical domains of the harvester, thus maximizing the scavenged power fed to the load.

If the mass of the beam is negligibly small with respect to the inertial mass m, the differential equation describing the

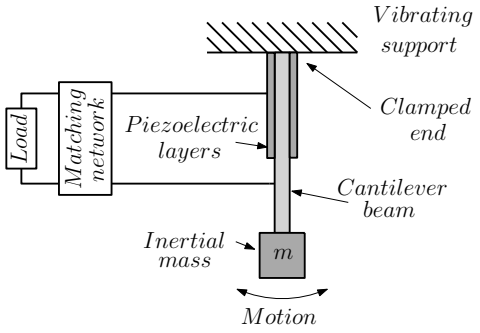

Fig. 1. Schematic representation of a piezoelectric energy harvester for ambient mechanical vibrations.

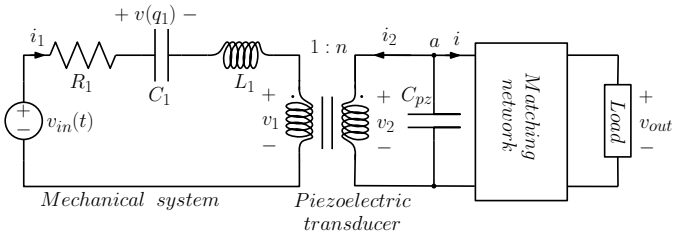

Fig. 2. Equivalent circuit for a piezoelectric energy harvester. The case of a linear elastic force is depicted here. In the general case, capacitance C_1 becomes nonlinear, along with the relation $v(q_1)$.

mechanical structure reads

$$m\frac{\mathrm{d}^2x}{\mathrm{d}t^2} + \frac{\mathrm{d}U(x)}{\mathrm{d}x} + \gamma\frac{\mathrm{d}x}{\mathrm{d}t} = f_{\text{ext}}(t) + f_{\text{pz}}(t) \tag{1}$$

where x is the beam displacement, $U(x)$ is the elastic potential of the beam, and γ is the friction constant. $f_{\text{ext}}(t)$ represents the external force describing vibrations, while $f_{\text{pz}}(t)$ is the feedback force applied to the mechanical part by the piezoelectric layers.

Concerning the piezoelectric transducer, the macro-scale equations can be put in the following form [15]

$$f_{\text{pz}} = -\theta v_2 \tag{2a}$$

$$q = \theta x - C_{\text{pz}} v_2 \tag{2b}$$

where θ is the electro-mechanical coupling constant (in N/V or As/m), v_2 is the voltage established across the transducer, q represent the corresponding electrical charge (so that $\mathrm{d}q/\mathrm{d}t = i$ becomes the current delivered by the transducer, see Fig. 2), and C_{pz} represents the piezoelectric capacitance.

An equivalent circuit representing the mechanical and mechanical-electrical transduction elements can be easily derived exploiting mechanical-to-electrical analogies, where position is replaced by a charge, mass by inductance, elastic stiffness by capacity, friction by resistance, and forces by voltages. The substitutions are summarized in Table I, where a linear elastic constant k is used (thus, a quadratic elastic potential $U(x)$ is assumed in (1)). The equivalent circuit is shown in figure 2.

TABLE I
MECHANICAL TO ELECTRICAL ANALOGIES

$x \to q_1$	$m \to L_1$	$f_{\text{ext}}(t) \to v_{\text{in}}(t)$
$\frac{\mathrm{d}x}{\mathrm{d}t} \to \frac{\mathrm{d}q_1}{\mathrm{d}t} = i_1$	$\gamma \to R$	$k \to C_1^{-1}$

Applying Kirchhoff voltage law (KVL) to the right loop, and Kirchhoff current law (KCL) to node a, the following differential equations are obtained

$$\frac{\mathrm{d}q_1}{\mathrm{d}t} = i_1 \tag{3a}$$

$$\frac{\mathrm{d}i_1}{\mathrm{d}t} = -\frac{1}{L_1}v(q_1) - \frac{R_1}{L_1}i_1 - \frac{1}{nL_1}v_2 + \frac{1}{L1}v_{\text{in}}(t) \tag{3b}$$

$$\frac{\mathrm{d}v_2}{\mathrm{d}t} = \frac{1}{nC_{\text{pz}}}i_1 - \frac{1}{C_{\text{pz}}}i \tag{3c}$$

where the elastic force has been been replaced by the voltage across the capacitor $v(q_1)$, and $n = \theta^{-1}$. It should be noted that the current i delivered by the harvester will depend on the matching network and on the load. Different configurations will be considered in the next section.

The voltage source $v_{\text{in}}(t)$ represents the random mechanical vibrations, and will be modelled here as a Gaussian white noise voltage source. Consequently, the differential equations (3) should be interpreted as stochastic differential equations (SDEs). We shall use the Itô interpretation[1]. Adopting the standard notation for Itô SDEs, the external voltage source will be written as

$$v_{\text{in}}(t)\mathrm{d}t = D\mathrm{d}W_t \tag{4}$$

where $D \in \mathbb{R}^+$ is a real positive parameter, W_t is a scalar Wiener process (the integral of a white noise), $\mathbb{E}[\mathrm{d}W_t] = 0$, $\mathbb{E}[\mathrm{d}W_t \mathrm{d}W_s] = \delta(t-s)$ and $\mathbb{E}[\cdot]$ denotes the expectation operator.

III. MATCHING NETWORK DESIGN AND COMPARISON

We show here that the harvested power and the power efficiency of the harvester can be maximized by the interposition of a second order matching network between the energy harvester and the load. To illustrate the result, we shall compare the performance of the proposed solution with both the simple resistive load, and with the power factor correction solution, consisting in placing a shunted reactive element in parallel with the load to compensate the reactive part of the equivalent impedance seen from the load [11], [12].

If nonlinear effects in the beam stiffness are neglected, the elastic potential reduces to $U(x) = kx^2/2$. Consequently, the equivalent circuit in figure 2 is linear, with a linear capacitor characterized by the voltage-charge characteristic $v(q_1) = q_1/C_1$, and it can be effectively analyzed in the frequency domain.

[1]As the forcing term in (3) is additive (i.e., not modulated), there is no Itô-Stratonovich interpretation dilemma [16].

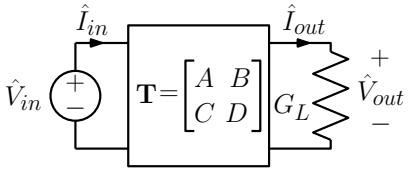

Fig. 3. Two port network closed on a resistive loop with conductance $G_L = R_L^{-1}$.

For a linear time invariant system (LTI) the input-output relation takes the form

$$y(t) = \int_{-\infty}^{+\infty} dr\, h(r)\, x(t-r) = h(t) * x(t) \tag{5}$$

where $h(t)$ is the step response, and $*$ denotes the convolution product. The autocorrelation function $R_{yy}(\tau)$ of the output variable $y(t)$ is given by [17]

$$\begin{aligned} R_{yy}(\tau) &= \mathbb{E}[y(t)y(t-\tau)] \\ &= \int_{-\infty}^{+\infty} dr \int_{-\infty}^{+\infty} ds\, h(r)\, h(s) R_{xx}(\tau + r - s) \end{aligned} \tag{6}$$

Taking the Fourier transform we obtain the well known relation between input and output power spectral densities

$$S_Y(\omega) = |H(\omega)|^2\, S_X(\omega) \tag{7}$$

where $H(\omega) = \hat{Y}(\omega)/\hat{X}(\omega)$ is the transfer function, and $\hat{Y}(\omega)$, $\hat{X}(\omega)$ are the Fourier transforms of $y(t)$ and $x(t)$, respectively. The total power is calculated by integrating the correspondent power spectral densities over the whole frequency spectrum. Using the properties of white Gaussian noise, it is straightforward to calculate the power spectral density for the mechanical vibrations

$$S_{\hat{V}_{\text{in}}}(\omega) = D^2 \tag{8}$$

which reflects the well known fact that energy content for white noise is constant over all frequencies. Obviously a true white noise signal cannot exist in the real world, as (8) would imply an infinite power content. Still, band-limited white noise, e.g. noise with flat spectrum within a frequency interval and null otherwise, is a realistic model for many noise sources.

We aim at comparing the harvested power for different matching networks. Therefore, it is convenient to view the equivalent circuit of figure 2, as composed by cascade interconnected two-port networks. Given a network composed by N cascade interconnected two-ports, each represented by a transmission matrix[2] $\mathbf{T_k}(\omega)$, the total transmission matrix is given by

$$\mathbf{T}(\omega) = \begin{bmatrix} A(\omega) & B(\omega) \\ C(\omega) & D(\omega) \end{bmatrix} = \prod_{k=1}^{N} \mathbf{T_k}(\omega) \tag{9}$$

[2]The transmission matrix is also known as $ABCD$ matrix. Symbol B should not be confused with the susceptance used later on.

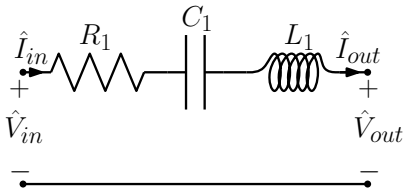

Fig. 4. Equivalent circuit for the mechanical domain.

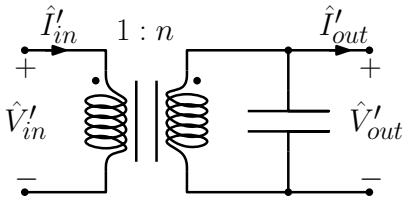

Fig. 5. Equivalent circuit for the piezoelectric transducer.

When the cascaded network is closed on a resistive load with conductance $G_L = R_L^{-1}$ as in figure 3, the transfer function $H(\omega) = \hat{V}_{\text{out}}(\omega)/\hat{V}_{\text{in}}(\omega)$ is easily found as

$$H(\omega) = \frac{\hat{V}_{\text{out}}(\omega)}{\hat{V}_{\text{in}}(\omega)} = (A(\omega) + B(\omega)G_L)^{-1} \tag{10}$$

The power absorbed by the conductance G_L is calculated substituting (10) into (7) and integrating over the whole frequency spectrum

$$P_{G_L} = G_L\, D^2 \int_{-\infty}^{+\infty} |H(\omega)|^2\, d\omega \tag{11}$$

In the frequency domain, the transmission parameter description for the mechanical part of the harvester, as shown in figure 4, is

$$\begin{bmatrix} \hat{V}_{\text{in}} \\ \hat{I}_{\text{in}} \end{bmatrix} = \underbrace{\begin{bmatrix} 1 & R_1 + jX_1(\omega) \\ 0 & 1 \end{bmatrix}}_{\mathbf{T}_{\text{M}}(\omega)} \begin{bmatrix} \hat{V}_{\text{out}} \\ \hat{I}_{\text{out}} \end{bmatrix} \tag{12}$$

where $j = \sqrt{-1}$, $X_1(\omega) = \omega L_1 - 1/(\omega C_1)$ is the reactance of the mechanical part, and $\mathbf{T}_{\text{M}}(\omega)$ is the mechanical transmission matrix.

Similarly, for the equivalent circuit of the piezoelectric transducer shown in figure 5, the transmission parameter representation is

$$\begin{bmatrix} \hat{V}'_{\text{in}} \\ \hat{I}'_{\text{in}} \end{bmatrix} = \underbrace{\begin{bmatrix} \frac{1}{n} & 0 \\ jnB_{\text{pz}}(\omega) & n \end{bmatrix}}_{\mathbf{T}_{\text{pz}}(\omega)} \begin{bmatrix} \hat{V}'_{\text{out}} \\ \hat{I}'_{\text{out}} \end{bmatrix} \tag{13}$$

where $B_{\text{pz}}(\omega) = \omega C_{\text{pz}}$ and $\mathbf{T}_{\text{pz}}(\omega)$ are the susceptance and the transmission matrix of the piezoelectric transducer, respectively.

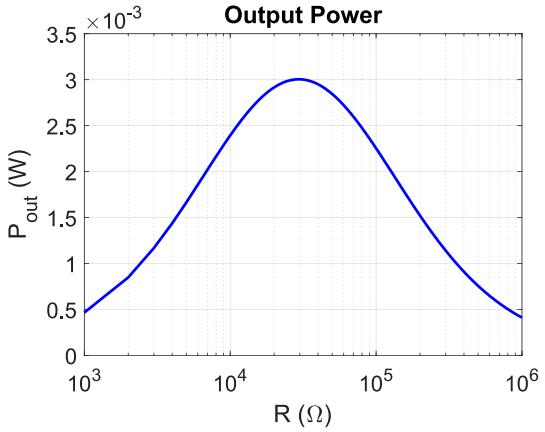

Fig. 6. Total harvested power for a piezoelectric energy harvester closed on a resistive load, as a function of the load resistance. Parameters' values are based on [18].

TABLE II
VALUES OF CIRCUIT COMPONENTS, BASED ON [18]

Parameter	Value
R_1	6.9366 Ω
C_1	5.874 μF
L_1	1 H
C_{pz}	80.08 nF
R_L	1 MΩ
n	37.4254
D	0.1 V

A. Resistive load

It is usually assumed that the load, modelled as a simple resistor, is directly connected to the output port of the piezoelectric transducer. If this is the case, the transmission matrix is $\mathbf{T}(\omega) = \mathbf{T}_{\text{M}}(\omega)\mathbf{T}_{\text{pz}}(\omega)$. Using equations (10)-(13), the transfer function becomes

$$H(\omega) = \frac{n}{1 + n^2(G_L + jB_{\text{pz}}(\omega))(R_1 + jX_1(\omega))} \tag{14}$$

The total power harvester by the resistive load is then computed using (11). The total harvester power as a function of the load resistance is shown in figure 6. The values of the components are summarized in table II.

B. Power factor correction network

Several works have shown the total harvested power can be increased using power factor correction [11], [12], [19]. In this approach, a shunted inductor is placed in parallel with the resistive load (see figure 7). The value of the shunted inductor, is determined in such a way, that the circuit composed by the piezoelectric transducer and the shunted inductor resonates at the same frequency of the mechanical part. Therefore, the whole energy harvester behaves as two coupled resonators with the same resonance frequency.

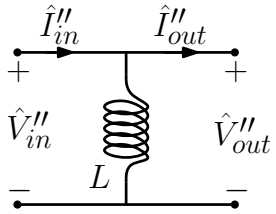

Fig. 7. Matching network for power factor correction.

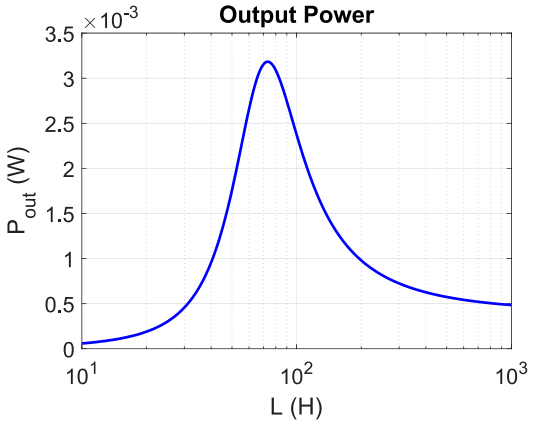

Fig. 8. Total harvested power for a piezoelectric energy harvester with a power factor correction matching network, as a function of the shunted inductance value L. Parameters' values are based on [18].

The transmission matrix for the shunted inductor in figure 7 is

$$\begin{bmatrix} \hat{V}''_{\text{in}} \\ \hat{I}''_{\text{in}} \end{bmatrix} = \underbrace{\begin{bmatrix} 1 & 0 \\ jB_{\text{L}}(\omega) & 1 \end{bmatrix}}_{\mathbf{T}_{\text{PF}}(\omega)} \begin{bmatrix} \hat{V}''_{\text{out}} \\ \hat{I}''_{\text{out}} \end{bmatrix} \tag{15}$$

where $B_{\text{L}} = -(\omega L)^{-1}$ is the inductor susceptance. The total transmission matrix is $\mathbf{T}(\omega) = \mathbf{T}_{\text{M}}(\omega)\,\mathbf{T}_{\text{pz}}(\omega)\,\mathbf{T}_{\text{PF}}(\omega)$ while the transfer function takes the form

$$H(\omega) = \frac{n}{1 + n^2(G_L + jB_2(\omega))(R_1 + jX_1(\omega))} \tag{16}$$

where $B_2(\omega) = \omega C_{\text{pz}} - (\omega L)^{-1}$. The value of the shunt inductor that maximize the harvested power turns out to be the resonant value $L_{\text{max}} = L_1 C_1 / C_{\text{pz}}$.

Figure 8 shows the total harvested power versus the shunted inductance value L. Values of the circuit parameters are taken from [18]. It should be noted that for the reference load resistance value $R_L = 1$ MΩ [18], application of the power factor correction network increases the harvested power with respect to a simple resistive load almost by a factor of 8 (see table III).

C. Low-pass L-matching network

The matching network proposed in this work, is a simple low-pass L-matching network, as shown in figure 9. In this matching setup two reactive elements, an inductor L and a capacitor C_P are arranged in a L-shaped structure. At very low frequencies, the inductor behaves as a short circuit, and

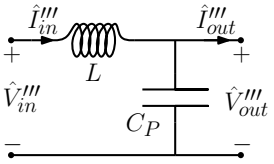

Fig. 9. L-matching low pass network.

TABLE III
MAXIMUM HARVESTED POWER FOR $R_L = 1\text{M}\Omega$

Resistive load	Power factor correction	L–matching
0.41059 mW	3.1834 mW	3.7261 mW

the capacitor as an open circuit. At very high frequencies the behavior is reversed, so that the network is a low-pass filter. It is worth mentioning that there exist many different matching network solutions, which differ for the number of components and for their topology. The aim of this work is to show that impedance matching can be an instrumental tool to increase the performance of energy harvesters, and therefore we restrict the attention to the simplest matching network.

For the low-pass L-matching network of figure 9, the transmission matrix takes the form

$$\begin{bmatrix} \hat{V}'''_{\text{in}} \\ \hat{I}'''_{\text{in}} \end{bmatrix} = \underbrace{\begin{bmatrix} 1 - X_L\,B_P & jX_L \\ jB_P(\omega) & 1 \end{bmatrix}}_{\mathbf{T}_{\text{mat}}(\omega)} \begin{bmatrix} \hat{V}'''_{\text{out}} \\ \hat{I}'''_{\text{out}} \end{bmatrix} \tag{17}$$

where $X_L = \omega L$ and $B_P = \omega C_P$. The total transmission matrix is $\mathbf{T}(\omega) = \mathbf{T}_{\text{M}}(\omega)\,\mathbf{T}_{\text{pz}}(\omega)\,\mathbf{T}_{\text{mat}}(\omega)$, and the transfer function is $H(\omega) = (n\Delta(\omega))^{-1}$, where (explicit dependence on ω is omitted for simplicity of notation)

$$\Delta(\omega) = \det \begin{bmatrix} R_1 + jX_1 & \frac{1}{n}(1 + jX_L(G_L + jB_P)) \\ -\frac{1}{n} & jB_{\text{pz}}(1 + jX_L(G_L + jB_P)) + G_L + jB_P \end{bmatrix} \tag{18}$$

Figure 10 shows the total harvested power for an energy harvester with the low-pass L-matching network, versus the values of the matching parameters L and C_P. In this example, maximum power is harvested for $L = 303.7273$ H and $C_P = 23.309$ nF. It should be noted that the unrealistically large value of the matching inductor is a consequence of the normalization adopted, i.e. of posing $L_1 = 1$ H.

The harvester with the low-pass L-matching network is capable to collect 9 times more power than the harvester with a simple resistive load, and 17% more power than the solution with the power factor correction matching network

Finally, figure 11 shows a comparison between the amplitude responses (i.e., $|H(\omega)|^2$) for the three different setups considered. Because the harvested power depends on the integral of the amplitude response, the design strategy is a trade-off between maximum amplitude, and passband width.

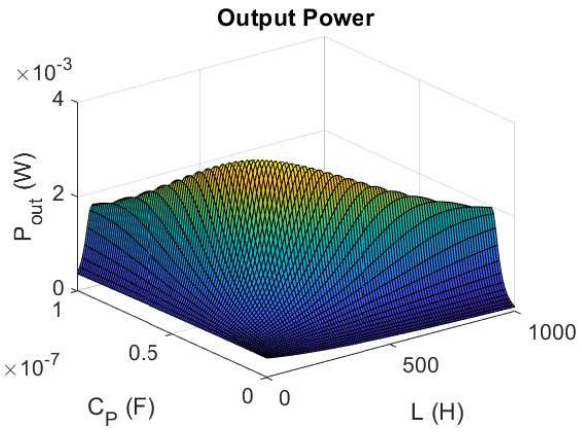

Fig. 10. Total harvested power for a piezoelectric energy harvester with a L-matching network, as a function of the matching parameters L and C_P. Parameters' values are based on [18].

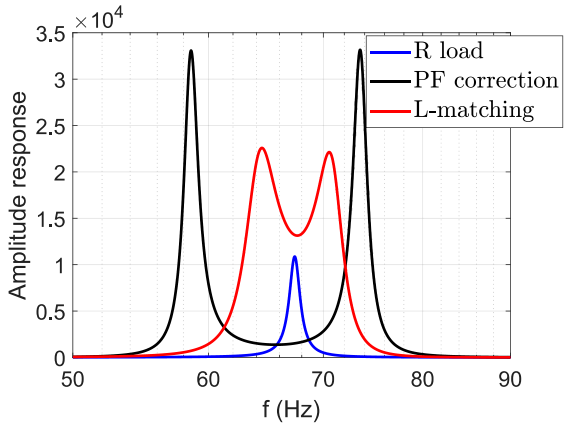

Fig. 11. Amplitude response ($|H(\omega)|^2$) as a function of frequency for the three setup considered: resistive load; power factor correction and low-pass L-matching network.

IV. Conclusions

In this contribution we have studied the impact of load matching to improve the power delivery capabilities of piezoelectric energy harvesters subject to Gaussian white random mechanical vibrations. Exploiting mechanical-to-electrical analogies, an equivalent circuit representing the entire Itô SDEs describing the harvester dynamics has been derived. This description enables the use of circuit theory approaches to the estimation of the power delivered to the load in presence of different types of two-port matching networks, namely the purely resistive load, the power factor correction solution, and the use of a simple, second order L–shaped low-pass matching network. We have shown that the latter architecture boosts the harvested power with respect to the simple, unmatched resistive load by a factor larger than 9, and with respect to the power factor correction solution by more than 17%.

References

[1] S. Roundy, P. K. Wright, and J. M. Rabaey, *Energy scavenging for wireless sensor networks*. Springer, 2003.

[2] S. P. Beeby, M. J. Tudor, and N. White, "Energy harvesting vibration sources for microsystems applications," *Measurement science and technology*, vol. 17, no. 12, p. R175, 2006.

[3] S. P. Beeby, R. Torah, M. Tudor, P. Glynne-Jones, T. O'donnell, C. Saha, and S. Roy, "A micro electromagnetic generator for vibration energy harvesting," *Journal of Micromechanics and microengineering*, vol. 17, no. 7, p. 1257, 2007.

[4] S. R. Anton and H. A. Sodano, "A review of power harvesting using piezoelectric materials (2003–2006)," *Smart materials and Structures*, vol. 16, no. 3, p. R1, 2007.

[5] K. Cook-Chennault, N. Thambi, and A. Sastry, "Powering mems portable devices. a review of non-regenerative and regenerative power supply systems with special emphasis on piezoelectric energy harvesting systems," *Smart Materials and Structures*, vol. 17, no. 4, p. 043001, 2008.

[6] A. Khaligh, P. Zeng, and C. Zheng, "Kinetic energy harvesting using piezoelectric and electromagnetic technologiesstate of the art," *IEEE transactions on industrial electronics*, vol. 57, no. 3, pp. 850–860, 2009.

[7] H. Vocca, I. Neri, F. Travasso, and L. Gammaitoni, "Kinetic energy harvesting with bistable oscillators," *Applied Energy*, vol. 97, pp. 771–776, 2012.

[8] X. Wen, W. Yang, Q. Jing, and Z. L. Wang, "Harvesting broadband kinetic impact energy from mechanical triggering/vibration and water waves," *ACS nano*, vol. 8, no. 7, pp. 7405–7412, 2014.

[9] Y. Fu, H. Ouyang, and R. B. Davis, "Nonlinear dynamics and triboelectric energy harvesting from a three-degree-of-freedom vibro-impact oscillator," *Nonlinear Dynamics*, vol. 92, no. 4, pp. 1985–2004, 2018.

[10] M. Bonnin, F. L. Traversa, and F. Bonani, "Analysis of influence of nonlinearities and noise correlation time in a single-dof energy-harvesting system via power balance description," *Nonlinear Dynamics*, vol. 100, no. 1, pp. 119–133, 2020.

[11] ——, "Leveraging circuit theory and nonlinear dynamics for the efficiency improvement of energy harvesting," *Nonlinear Dynamics*, vol. 104, no. 1, pp. 367–382, 2021.

[12] ——, "On the application of circuit theory and nonlinear dynamics to the design of highly efficient energy harvesting systems," in *2021 International Conference on Smart Energy Systems and Technologies (SEST)*. IEEE, 6–8 sep 2021.

[13] ——, "An impedance matching solution to increase the harvested power and efficiency of nonlinear piezoelectric energy harvesters," *Energies*, vol. 15, p. 2764, 2022.

[14] L. Gammaitoni, "There's plenty of energy at the bottom (micro and nano scale nonlinear noise harvesting)," *Contemporary Physics*, vol. 53, no. 2, pp. 119–135, 2012.

[15] S. Priya and D. J. Inman, *Energy harvesting technologies*. Springer, 2009, vol. 21.

[16] B. Øksendal, *Stochastic Differential Equations*, 6th ed. Berlin: Springer–Verlag, 2003.

[17] C. W. Gardiner *et al.*, *Handbook of stochastic methods*. Springer Berlin, 1985, vol. 3.

[18] Y. Yang and L. Tang, "Equivalent circuit modeling of piezoelectric energy harvesters," *Journal of intelligent material systems and structures*, vol. 20, no. 18, pp. 2223–2235, 2009.

[19] T. Yu and S. Zhou, "Performance investigations of nonlinear piezoelectric energy harvesters with a resonant circuit under white gaussian noises," *Nonlinear Dynamics*, vol. 103, no. 1, pp. 183–196, 2021.